EUROPEAN ORGANIZATION FOR NUCLEAR RESEARCH

CERN-EP/2000-135
November 6, 2000

$K^0_S K^0_S$ Final State in Two-Photon Collisions and Implications for Glueballs

The L3 Collaboration

Abstract

The $K^0_S K^0_S$ final state in two-photon collisions is studied with the L3 detector at LEP. The mass spectrum is dominated by the formation of the $f'_2(1525)$ tensor meson in the helicity-two state with a two-photon width times the branching ratio into $K\bar{K}$ of $76 \pm 6 \pm 11$ eV. A clear signal for the formation of the $f_J(1710)$ is observed and it is found to be dominated by the spin-two helicity-two state. No resonance is observed in the mass region around 2.2 GeV and an upper limit of 1.4 eV at 95% C.L. is derived for the two-photon width times the branching ratio into $K^0_S K^0_S$ for the glueball candidate $\xi(2230)$.

Dedicated to the memory of Prof. Bianca Monteleoni

Submitted to *Phys. Lett. B*

1 Introduction

The formation of resonances in two-photon collisions is studied via the process $e^+e^- \to e^+e^-\gamma^*\gamma^* \to e^+e^-R \to e^+e^-K^0_SK^0_S$, where γ^* is a virtual photon. The outgoing electron and positron carry nearly the full beam energy and their transverse momenta are usually so small that they are not detected. In this case the two photons are quasi-real. The cross section for this process is given by the convolution of the QED calculable luminosity function $\mathcal{L}_{\gamma\gamma}$, giving the flux of the photons, with a Breit-Wigner function. This leads to the proportionality relation between the measured cross section and the two-photon width $\Gamma_{\gamma\gamma}(R)$ of the resonance R

$$\sigma(e^+e^- \to e^+e^-R) = \mathcal{K} \cdot \Gamma_{\gamma\gamma}(R), \tag{1}$$

where the proportionality factor $\mathcal{K}$ is evaluated by a Monte Carlo integration.

The quantum numbers of the resonance must be compatible with the initial state of the two quasi-real photons. A neutral, unflavoured meson with even charge conjugation, J≠1 and helicity-zero (λ=0) or two (λ=2) can be formed. In order to decay into $K^0_SK^0_S$, a resonance must have $J^{PC} = (\text{even})^{++}$. For the 2^{++}, 1^3P_2 tensor meson nonet, the $f_2(1270)$, the $a^0_2(1320)$ and the $f'_2(1525)$ can be formed. However, since these three states are close in mass, interferences must be taken into account. The $f_2(1270)$ interferes constructively with the $a^0_2(1320)$ in the K^+K^- final state but destructively in the $K^0\bar{K}^0$ final state [1].

Gluonium states cannot be formed directly by the collision of two photons and the two-photon width of a glueball is expected to be very small. A state that is observed in a gluon rich environment but not in two photon fusion has the typical signature of a glueball.

The data used for this analysis correspond to an integrated luminosity of $588\,\text{pb}^{-1}$ collected by the L3 detector [2] at LEP around the Z pole ($143\,\text{pb}^{-1}$) and at high energies, $\sqrt{s} = 183 - 202$ GeV ($445\,\text{pb}^{-1}$). The $K^0_SK^0_S$ final state in two-photon collisions was studied by L3 [3] with a luminosity of $114\,\text{pb}^{-1}$ and by TASSO, PLUTO and CELLO at lower energies and luminosities at PETRA [4].

The EGPC [5] Monte Carlo generator is used to describe two-photon resonance formation. The generator is based on the formalism of Reference 6. All the generated events are passed through the full detector simulation program based on GEANT [7] and GHEISHA [8] and are reconstructed following the same procedure used for the data. Time dependent detector inefficiencies, as monitored during the data taking period, are also simulated.

2 Event selection

The selection of exclusive $K^0_SK^0_S$ events is based on the decay $K^0_S \to \pi^+\pi^-$, exploiting the central tracking system and the electromagnetic calorimeter. The events are collected predominantly by the charged particle track triggers [9]. In order to select $e^+e^- \to e^+e^-\pi^+\pi^-\pi^+\pi^-$ events, we require:

- The total energy seen in the calorimeters must be smaller than 30 GeV to exclude annihilation events.
- There must be exactly four charged tracks in the tracking chamber with a net charge of zero, a polar angle θ in the range $24^\circ < \theta < 156^\circ$ and a transverse momentum greater than 100 MeV.

The K^0_S's are identified by secondary vertex reconstruction. The $\pi^+\pi^-$ mass distribution is shown in Figure 1a where a mass resolution $\sigma = 8.0 \pm 0.5$ MeV is found, consistent with the Monte Carlo simulation.

In order to select $K^0_S K^0_S$ exclusive events, we require:

- The total transverse momentum imbalance squared $|\sum \overrightarrow{p_T}|^2$ must be less than 0.1 GeV^2. In Figure 1b the $|\sum \overrightarrow{p_T}|^2$ distribution is compared to the Monte Carlo prediction for exclusive $K^0_S K^0_S$ formation. The excess in the data at high values is due to non-exclusive final states.

- No photons. A photon is defined as an isolated shower in the electromagnetic calorimeter with a total energy larger than 100 MeV distributed in more than two crystals. The ratio between the energies deposited in the hadronic and electromagnetic calorimeters must be less than 0.2 and there must be no charged track within 200 mrad from the shower direction.

- Two secondary vertices with transverse distances from the interaction point greater than 1 mm and 3 mm. In Figure 1c the data are compared to the Monte Carlo prediction for exclusive $K^0_S K^0_S$ formation. The excess in the data at low values is due to the dominant $\gamma\gamma \to \rho^0\rho^0$ channel.

- The angle between the flight direction of each K^0_S candidate and the total transverse momentum vector of the two outgoing tracks in the transverse plane must be less than 0.3 rad, as presented in Figure 1d.

- Since the two K^0_S's are produced back-to-back in the transverse plane, the angle between the flight directions of the two K^0_S candidates in this plane is required to be $\pi \pm 0.3$ rad.

Figure 2 shows the distribution of the mass of one K^0_S candidate versus the mass of the other candidate. There is a strong enhancement corresponding to the $K^0_S K^0_S$ exclusive formation over a small background. We require that the invariant masses of the two K^0_S candidates must be inside a circle of 40 MeV radius centred on the peak of the $K^0_S K^0_S$ signal.

With these selection criteria, 802 events are found in the data sample. The background due to misidentified K^0_S pairs and non-exclusive events is estimated to be less than 5% by a study of the K^0_S mass sidebands and of the $|\sum \overrightarrow{p_T}|^2$ distribution. The backgrounds due to $K^0_S K^\pm \pi^\mp$ and $\Lambda\bar{\Lambda}$ final states and to beam-gas and beam-wall interactions are found to be negligible.

3 The $K^0_S K^0_S$ mass spectrum

The $K^0_S K^0_S$ mass spectrum is presented in Figure 3 showing three distinct peaks over a low background. Despite their large two-photon widths, the $f_2(1270)$ and the $a^0_2(1320)$ tensor mesons produce a small signal in the $K^0_S K^0_S$ final state due to their destructive interference. The spectrum is dominated by the formation of the $f'_2(1525)$ tensor meson in agreement with previous observations [3, 4]. A signal for the formation of the $f_J(1710)$ is present while no resonance is observed in the mass region of the $\xi(2230)$.

A maximum likelihood fit using three Breit-Wigner functions plus a second order polynomial for the background is performed on the full $K^0_S K^0_S$ mass spectrum. The results of the fit are shown in Figure 3 and reported in Table 1. The confidence level is 31.7%. The parameters of the $f'_2(1525)$ are in good agreement with the PDG [10], taking into account the experimental resolution $\sigma = 29 \pm 4$ MeV.

4 The $f_2'(1525)$ tensor meson

To study the $f_2'(1525)$ tensor meson Monte Carlo events are generated according to the mass, total width and two-photon width [10] of this state. The angular distribution of the two K_S^0's in the two-photon centre of mass system is generated uniformly in $\cos\theta^*$ and in ϕ^*, the polar and azimuthal angles defined by the beam line. In order to take into account the helicity of a spin-two resonance, a weight w is assigned to each generated event: $w = (\cos^2\theta^* - \frac{1}{3})^2$ for spin-two helicity-zero (J=2, λ=0) and $w = \sin^4\theta^*$ for spin-two helicity-two (J=2, λ=2).

To determine the spin and the helicity composition in the $f_2'(1525)$ mass region between 1400 and 1640 MeV, the experimental polar angle distribution is compared with the normalized Monte Carlo expectations for the (J=0), (J=2, λ=0) and (J=2, λ=2) states, as presented in Figure 4. A χ^2 is calculated for each hypothesis, after grouping bins in order to have at least 10 entries both in the data and in the Monte Carlo. The confidence levels for the (J=0) and (J=2, λ=0) hypotheses are less then 10^{-6}. For the (J=2, λ=2) hypothesis, a confidence level of 99.9% is obtained. The contributions of (J=0) and (J=2, λ=0) are found to be compatible with zero when fitting the three waves simultaneously. The contribution of (J=2, λ=2) is found to be compatible with unity within 7%, in agreement with theoretical predictions [11].

The two-photon width times the branching ratio into $K\bar{K}$ is therefore determined from the cross section under the hypothesis of a pure (J=2, λ=2) state. Two separate measurements are performed for data collected at the Z pole and at high energies. The $\mathcal{K}$ factor, the total detection efficiency and the measured quantity $\Gamma_{\gamma\gamma}(f_2'(1525)) \times \mathrm{Br}(f_2'(1525) \to K\bar{K})$ are reported in Table 2. The total detection efficiency, ε, is determined by Monte Carlo and includes detector acceptance, trigger efficiency and selection criteria. Combining the two measurements, the value

$$\Gamma_{\gamma\gamma}\Big(f_2'(1525)\Big) \times \mathrm{Br}\Big(f_2'(1525) \to K\bar{K}\Big) = 76 \pm 6 \pm 11 \text{ eV}$$

is obtained, where the first uncertainty is statistical and the second is systematic. The main source of systematic uncertainty comes from the fitting procedure. A contribution of 10% is evaluated by varying the shape of the background and by allowing no background at all. Other sources of systematic uncertainties are trigger efficiency (5%) and cut variations (7%). This result agrees with and supersedes the value previously published by L3 [3].

5 The 1750 MeV mass region

According to lattice QCD predictions [12], the ground state glueball has $J^{PC} = 0^{++}$ and a mass between 1400 and 1800 MeV. Several 0^{++} states are observed in this mass region [10] and the scalar ground state glueball can mix with nearby quarkonia [13].

To investigate the spin composition in the mass region of the $f_J(1710)$, the angular distribution of the two K_S^0's is studied in the mass region between 1640 and 2000 MeV. A resonance with a mass of 1750 MeV and a total width of 200 MeV is generated as for the $f_2'(1525)$. The detection efficiencies for the various spin and helicity hypotheses are reported in Table 3.

A fit of the angular distribution is performed using a combination of the two waves (J=0) and (J=2, λ=2) for the signal plus the distribution of the tail of the $f_2'(1525)$. Contributions from the (J=2, λ=0) wave are not considered, based on the theoretical predictions [11] and our experimental results for the $f_2'(1525)$. The tail of the $f_2'(1525)$ is modeled by assuming a pure (J=2, λ=2) state. The fraction of the events belonging to the $f_2'(1525)$ in the 1750 MeV mass region is found to be 14%. The fit results are shown in Figure 5. The confidence level for the fit

is 68.0% whereas the (J=0) fraction is 24±16%. Neglecting the (J=0) wave yields a confidence level of 24.0%. The possible (J=2, λ=0) contribution is found to be compatible with zero. The (J=2, λ=2) wave is found to be dominant and the two-photon width measured in the full data sample is

$$\Gamma_{\gamma\gamma}\Big(\mathrm{f_2}(1750)\Big) \times \mathrm{Br}\Big(\mathrm{f_2}(1750) \to \mathrm{K\bar{K}}\Big) = 49 \pm 11 \pm 13 \text{ eV}.$$

The systematic uncertainty takes into account the selection criteria, the trigger efficiency, the fitting procedure, the uncertainty on the total width and on the (J=2, λ=2) fraction.

The (J=2, λ=2) signal may be due to the formation of the first radial excitation of a tensor meson state, predicted at a mass of 1740 MeV [14,15] with a two-photon width of 1.04 keV [14]. The BES Collaboration reported the presence of both 2^{++} and 0^{++} waves in the 1750 MeV mass region in $\mathrm{K^+K^-}$ in the reaction $\mathrm{e^+e^-} \to \mathrm{J} \to \mathrm{K^+K^-}\gamma$ [16]. Their (J=0) fraction is estimated to be 30±10%, in good agreement with our measurement.

6 The 2230 MeV mass region

The $\xi(2230)$ is considered a good candidate for the ground state tensor glueball because of its narrow width and its production in a gluon rich environment. Its mass is in agreement with the lattice QCD predictions [12]. It was first observed in the radiative decays of the J particle by Mark III [17] and confirmed by BES [18].

Since gluons do not couple directly to photons, the two-photon width is expected to be small for a glueball, as quantified by the stickiness [19] defined as

$$\frac{|<\mathrm{R}|\mathrm{gg}>|^2}{|<\mathrm{R}|\gamma\gamma>|^2} \sim S_\mathrm{R} = N_l \left(\frac{m_\mathrm{R}}{k_{J\to\gamma\mathrm{R}}}\right)^{2l+1} \frac{\Gamma(\mathrm{J}\to\gamma\mathrm{R})}{\Gamma(\mathrm{R}\to\gamma\gamma)} \qquad (2)$$

where m_R is the mass of the state R, $k_{J\to\gamma\mathrm{R}}$ is the energy of the photon from a radiative J decay in the J rest frame and l is the orbital angular momentum between the two gluons. For spin-two states $l = 0$. The normalization factor N_l is calculated assuming the stickiness of the $\mathrm{f_2}(1270)$ tensor meson to be 1.

A Monte Carlo simulation is used to determine the detection efficiency for the $\xi(2230)$ using a mass of 2230 MeV and a total width of 20 MeV. A mass resolution of σ = 60 MeV is estimated. The total detection efficiency is reported in Table 4 for the two data samples, under the hypothesis of a pure (J=2, λ=2) state. The signal region is chosen to be $\pm 2\sigma$ around the $\xi(2230)$ mass. In order to evaluate the background two sidebands of 2σ each are considered. The number of events in the signal region and the expected background evaluated with a linear fit in the sideband region are reported in Table 4. Using a Poisson distribution with background [20] and combining the results for the two data samples, we obtain the upper limit

$$\Gamma_{\gamma\gamma}\Big(\xi(2230)\Big) \times \mathrm{Br}\Big(\xi(2230) \to \mathrm{K^0_S K^0_S}\Big) < 1.4 \text{ eV at 95\% C.L.},$$

under the hypothesis of a pure helicity-two state.

This translates, following Equation 2 and using world average values [10], into a lower limit on the stickiness $S_{\xi(2230)}$ of 74 at 95% C.L., similar to the results obtained by CLEO [21]. This value of the stickiness is much larger than the values measured for the well established $\mathrm{q\bar{q}}$ states and supports the interpretation of the $\xi(2230)$ as the tensor glueball.

Acknowledgements

We wish to express our gratitude to the CERN accelerator divisions for the excellent performance of the LEP machine. We acknowledge the contributions of the engineers and technicians who have participated in the construction and maintenance of this experiment.

References

[1] H. J. Lipkin, Nucl. Phys. **B 7** (1968) 321;
D. Faiman *et al.*, Phys. Lett. **B 59** (1975) 269.

[2] L3 Collab., B. Adeva *et al.*, Nucl. Inst. Meth. **A 289** (1990) 35;
L3 Collab., O. Adriani *et al.*, Phys. Rep. **236** (1993) 1;
M. Chemarin *et al.*, Nucl. Inst. Meth. **A 349** (1994) 345;
M. Acciarri *et al.*, Nucl. Inst. Meth. **A 351** (1994) 300;
I. C. Brock *et al.*, Nucl. Inst. Meth. **A 381** (1996) 236;
A. Adam *et al.*, Nucl. Inst. Meth. **A 383** (1996) 342.

[3] L3 Collab., M. Acciarri *et al.*, Phys. Lett. **B 363** (1995) 118.

[4] TASSO Collab., M. Althoff *et al.*, Phys. Lett. **B 121** (1982) 216;
TASSO Collab., M. Althoff *et al.*, Z. Phys. **C 29** (1985) 189;
PLUTO Collab., C. Berger *et al.*, Z. Phys. **C 37** (1988) 329;
CELLO Collab., H. J. Behrend *et al.*, Z. Phys. **C 43** (1989) 91.

[5] F. L. Linde, *Charm Production in Two-Photon Collisions*, Ph. D. Thesis, Rijksuniversiteit Leiden (1988).

[6] V. M. Budnev *et al.*, Phys. Rep. **C 15** (1975) 181.

[7] R. Brun *et al.*, GEANT 3.15 preprint CERN DD/EE/84-1 (1984); Revised 1987.

[8] H. Fesefeldt, RWTH Aachen report PITHA 85/2 (1985).

[9] P. Béné *et al.*, Nucl. Inst. Meth. **A 306** (1991) 150;
D. Haas *et al.*, Nucl. Inst. Meth. **A 420** (1999) 101.

[10] Particle Data Group, D. E. Groom *et al.*, Eur. Phys. J. **C 15** (2000) 1.

[11] B. Schrempp-Otto *et al.*, Phys. Lett. **B 36** (1971) 463;
G. Köpp *et al.*, Nucl. Phys. **B 70** (1974) 461;
P. Grassberger and R. Kögerler, Nucl. Phys. **B 106** (1976) 451.

[12] C. Michael, Nucl. Phys. **A 655** (1999) 12, and references therein.

[13] C. Amsler and F. E. Close, Phys. Lett. **B 353** (1995) 385;
C. Amsler and F. E. Close, Phys. Rev. **D 53** (1996) 295;
P. Minkowski and W. Ochs, Eur. Phys. J. **C 9** (2000) 283;
V. Ableev *et al.*, Nucl. Phys. **B 86** (2000) 351.

[14] C. R. Münz, Nucl. Phys. **A 609** (1996) 364.

[15] L. S. Celenza *et al.*, Phys. Rev. **C 60** (1999) 035206.

[16] BES Collab., J. Z. Bai *et al.*, Phys. Rev. Lett. **77** (1996) 3959.

[17] Mark III Collab., R. M. Baltrusaitis *et al.*, Phys. Rev. Lett. **56** (1986) 107.

[18] BES Collab., J. Z. Bai *et al.*, Phys. Rev. Lett. **76** (1996) 3502.

[19] M. Chanowitz, *Resonances in Photon-Photon Scattering*, Proceedings of the VIth International Workshop on Photon-Photon Collisions, World Scientific (1984).

[20] O. Helene, Nucl. Inst. Meth. **212** (1983) 319.

[21] CLEO Collab., R. Godang *et al.*, Phys. Rev. Lett. **79** (1997) 3829;
CLEO Collab., M. S. Alam *et al.*, Phys. Rev. Lett. **81** (1998) 3328.

The L3 Collaboration:

M.Acciarri,[26] P.Achard,[19] O.Adriani,[16] M.Aguilar-Benitez,[25] J.Alcaraz,[25] G.Alemanni,[22] J.Allaby,[17] A.Aloisio,[28] M.G.Alviggi,[28] G.Ambrosi,[19] H.Anderhub,[48] V.P.Andreev,[6,36] T.Angelescu,[12] F.Anselmo,[9] A.Arefiev,[27] T.Azemoon,[3] T.Aziz,[10] P.Bagnaia,[35] A.Bajo,[25] L.Baksay,[43] A.Balandras,[4] S.V.Baldew,[2] S.Banerjee,[10] Sw.Banerjee,[10] A.Barczyk,[48,46] R.Barillère,[17] P.Bartalini,[22] M.Basile,[9] N.Batalova,[45] R.Battiston,[32] A.Bay,[22] F.Becattini,[16] U.Becker,[14] F.Behner,[48] L.Bellucci,[16] R.Berbeco,[3] J.Berdugo,[25] P.Berges,[14] B.Bertucci,[32] B.L.Betev,[48] S.Bhattacharya,[10] M.Biasini,[32] A.Biland,[48] J.J.Blaising,[4] S.C.Blyth,[33] G.J.Bobbink,[2] A.Böhm,[1] L.Boldizsar,[13] B.Borgia,[35] D.Bourilkov,[48] M.Bourquin,[19] S.Braccini,[19] J.G.Branson,[39] F.Brochu,[4] A.Buffini,[16] A.Buijs,[44] J.D.Burger,[14] W.J.Burger,[32] X.D.Cai,[14] M.Capell,[14] G.Cara Romeo,[9] G.Carlino,[28] A.M.Cartacci,[16] J.Casaus,[25] G.Castellini,[16] F.Cavallari,[35] N.Cavallo,[37] C.Cecchi,[32] M.Cerrada,[25] F.Cesaroni,[23] M.Chamizo,[19] Y.H.Chang,[50] U.K.Chaturvedi,[18] M.Chemarin,[24] A.Chen,[50] G.Chen,[7] G.M.Chen,[7] H.F.Chen,[20] H.S.Chen,[7] G.Chiefari,[28] L.Cifarelli,[38] F.Cindolo,[9] C.Civinini,[16] I.Clare,[14] R.Clare,[14] G.Coignet,[4] N.Colino,[25] S.Costantini,[5] F.Cotorobai,[12] B.de la Cruz,[25] A.Csilling,[13] S.Cucciarelli,[32] T.S.Dai,[14] J.A.van Dalen,[30] R.D'Alessandro,[16] R.de Asmundis,[28] P.Déglon,[19] A.Degré,[4] K.Deiters,[46] D.della Volpe,[28] E.Delmeire,[19] P.Denes,[34] F.DeNotaristefani,[35] A.De Salvo,[48] M.Diemoz,[35] M.Dierckxsens,[2] D.van Dierendonck,[2] C.Dionisi,[35] M.Dittmar,[48] A.Dominguez,[39] A.Doria,[28] M.T.Dova,[18,♯] D.Duchesneau,[4] D.Dufournaud,[4] P.Duinker,[2] I.Duran,[40] H.El Mamouni,[24] A.Engler,[33] F.J.Eppling,[14] F.C.Erné,[2] P.Extermann,[19] M.Fabre,[46] M.A.Falagan,[25] S.Falciano,[35,17] A.Favara,[17] J.Fay,[24] O.Fedin,[36] M.Felcini,[48] T.Ferguson,[33] H.Fesefeldt,[1] E.Fiandrini,[32] J.H.Field,[19] F.Filthaut,[17] P.H.Fisher,[14] I.Fisk,[39] G.Forconi,[14] K.Freudenreich,[48] C.Furetta,[26] Yu.Galaktionov,[27,14] S.N.Ganguli,[10] P.Garcia-Abia,[5] M.Gataullin,[31] S.S.Gau,[11] S.Gentile,[35,17] N.Gheordanescu,[12] S.Giagu,[35] Z.F.Gong,[20] G.Grenier,[24] O.Grimm,[48] M.W.Gruenewald,[8] M.Guida,[38] R.van Gulik,[2] V.K.Gupta,[34] A.Gurtu,[10] L.J.Gutay,[45] D.Haas,[5] A.Hasan,[29] D.Hatzifotiadou,[9] T.Hebbeker,[8] A.Hervé,[17] P.Hidas,[13] J.Hirschfelder,[33] H.Hofer,[48] G. Holzner,[48] H.Hoorani,[33] S.R.Hou,[50] Y.Hu,[30] I.Iashvili,[47] B.N.Jin,[7] L.W.Jones,[3] P.de Jong,[2] I.Josa-Mutuberría,[25] R.A.Khan,[18] M.Kaur,[18,◇] M.N.Kienzle-Focacci,[19] D.Kim,[35] J.K.Kim,[42] J.Kirkby,[17] D.Kiss,[13] W.Kittel,[30] A.Klimentov,[14,27] A.C.König,[30] M.Kopal,[45] A.Kopp,[47] V.Koutsenko,[14,27] M.Kräber,[48] R.W.Kraemer,[33] W.Krenz,[1] A.Krüger,[47] A.Kunin,[14,27] P.Ladron de Guevara,[25] I.Laktineh,[24] G.Landi,[16] M.Lebeau,[17] A.Lebedev,[14] P.Lebrun,[24] P.Lecomte,[48] P.Lecoq,[17] P.Le Coultre,[48] H.J.Lee,[8] J.M.Le Goff,[17] R.Leiste,[47] P.Levtchenko,[36] C.Li,[20] S.Likhoded,[47] C.H.Lin,[50] W.T.Lin,[50] F.L.Linde,[2] L.Lista,[28] Z.A.Liu,[7] W.Lohmann,[47] E.Longo,[35] Y.S.Lu,[7] K.Lübelsmeyer,[1] C.Luci,[17,35] D.Luckey,[14] L.Lugnier,[24] L.Luminari,[35] W.Lustermann,[48] W.G.Ma,[20] M.Maity,[10] L.Malgeri,[17] A.Malinin,[17] C.Maña,[25] D.Mangeol,[30] J.Mans,[34] G.Marian,[15] J.P.Martin,[24] F.Marzano,[35] K.Mazumdar,[10] R.R.McNeil,[6] S.Mele,[17] L.Merola,[28] M.Meschini,[16] W.J.Metzger,[30] M.von der Mey,[1] A.Mihul,[12] H.Milcent,[17] G.Mirabelli,[35] J.Mnich,[1] G.B.Mohanty,[10] T.Moulik,[10] G.S.Muanza,[24] A.J.M.Muijs,[2] B.Musicar,[39] M.Musy,[35] M.Napolitano,[28] F.Nessi-Tedaldi,[48] H.Newman,[31] T.Niessen,[1] A.Nisati,[35] H.Nowak,[47] R.Ofierzynski,[48] G.Organtini,[35] A.Oulianov,[27] C.Palomares,[25] D.Pandoulas,[1] S.Paoletti,[35,17] P.Paolucci,[28] R.Paramatti,[35] H.K.Park,[33] I.H.Park,[42] G.Passaleva,[17] S.Patricelli,[28] T.Paul,[11] M.Pauluzzi,[32] C.Paus,[17] F.Pauss,[48] M.Pedace,[35] S.Pensotti,[26] D.Perret-Gallix,[4] B.Petersen,[30] D.Piccolo,[28] F.Pierella,[9] M.Pieri,[16] P.A.Piroué,[34] E.Pistolesi,[26] V.Plyaskin,[27] M.Pohl,[19] V.Pojidaev,[27,16] H.Postema,[14] J.Pothier,[17] D.O.Prokofiev,[45] D.Prokofiev,[36] J.Quartieri,[38] G.Rahal-Callot,[48,17] M.A.Rahaman,[10] P.Raics,[15] N.Raja,[10] R.Ramelli,[48] P.G.Rancoita,[26] R.Ranieri,[16] A.Raspereza,[47] G.Raven,[39] P.Razis,[29] D.Ren,[48] M.Rescigno,[35] S.Reucroft,[11] S.Riemann,[47] K.Riles,[3] J.Rodin,[43] B.P.Roe,[3] L.Romero,[25] A.Rosca,[8] S.Rosier-Lees,[4] J.A.Rubio,[17] G.Ruggiero,[16] H.Rykaczewski,[48] S.Saremi,[6] S.Sarkar,[35] J.Salicio,[17] E.Sanchez,[17] M.P.Sanders,[30] C.Schäfer,[17] V.Schegelsky,[36] S.Schmidt-Kaerst,[1] D.Schmitz,[1] H.Schopper,[49] D.J.Schotanus,[30] G.Schwering,[1] C.Sciacca,[28] A.Seganti,[9] L.Servoli,[32] S.Shevchenko,[31] N.Shivarov,[41] V.Shoutko,[27] E.Shumilov,[27] A.Shvorob,[31] T.Siedenburg,[1] D.Son,[42] B.Smith,[33] P.Spillantini,[16] M.Steuer,[14] D.P.Stickland,[34] A.Stone,[6] B.Stoyanov,[41] A.Straessner,[1] K.Sudhakar,[10] G.Sultanov,[18] L.Z.Sun,[20] S.Sushkov,[8] H.Suter,[48] J.D.Swain,[18] Z.Szillasi,[43,¶] T.Sztaricskai,[43,¶] X.W.Tang,[7] L.Tauscher,[5] L.Taylor,[11] B.Tellili,[24] C.Timmermans,[30] Samuel C.C.Ting,[14] S.M.Ting,[14] S.C.Tonwar,[10] J.Tóth,[13] C.Tully,[17] K.L.Tung,[7] Y.Uchida,[14] J.Ulbricht,[48] E.Valente,[35] G.Vesztergombi,[13] I.Vetlitsky,[27] D.Vicinanza,[38] G.Viertel,[48] S.Villa,[11] M.Vivargent,[4] S.Vlachos,[5] I.Vodopianov,[36] H.Vogel,[33] H.Vogt,[47] I.Vorobiev,[33] A.A.Vorobyov,[36] A.Vorvolakos,[29] M.Wadhwa,[5] W.Wallraff,[1] M.Wang,[14] X.L.Wang,[20] Z.M.Wang,[20] A.Weber,[1] M.Weber,[1] P.Wienemann,[1] H.Wilkens,[30] S.X.Wu,[14] S.Wynhoff,[17] L.Xia,[31] Z.Z.Xu,[20] J.Yamamoto,[3] B.Z.Yang,[20] C.G.Yang,[7] H.J.Yang,[7] M.Yang,[7] J.B.Ye,[20] S.C.Yeh,[51] An.Zalite,[36] Yu.Zalite,[36] Z.P.Zhang,[20] G.Y.Zhu,[7] R.Y.Zhu,[31] A.Zichichi,[9,17,18] G.Zilizi,[43,¶] B.Zimmermann,[48] M.Zöller.[1]

1 I. Physikalisches Institut, RWTH, D-52056 Aachen, FRG[§]
III. Physikalisches Institut, RWTH, D-52056 Aachen, FRG[§]
2 National Institute for High Energy Physics, NIKHEF, and University of Amsterdam, NL-1009 DB Amsterdam, The Netherlands
3 University of Michigan, Ann Arbor, MI 48109, USA
4 Laboratoire d'Annecy-le-Vieux de Physique des Particules, LAPP,IN2P3-CNRS, BP 110, F-74941 Annecy-le-Vieux CEDEX, France
5 Institute of Physics, University of Basel, CH-4056 Basel, Switzerland
6 Louisiana State University, Baton Rouge, LA 70803, USA
7 Institute of High Energy Physics, IHEP, 100039 Beijing, China[△]
8 Humboldt University, D-10099 Berlin, FRG[§]
9 University of Bologna and INFN-Sezione di Bologna, I-40126 Bologna, Italy
10 Tata Institute of Fundamental Research, Bombay 400 005, India
11 Northeastern University, Boston, MA 02115, USA
12 Institute of Atomic Physics and University of Bucharest, R-76900 Bucharest, Romania
13 Central Research Institute for Physics of the Hungarian Academy of Sciences, H-1525 Budapest 114, Hungary[‡]
14 Massachusetts Institute of Technology, Cambridge, MA 02139, USA
15 KLTE-ATOMKI, H-4010 Debrecen, Hungary[¶]
16 INFN Sezione di Firenze and University of Florence, I-50125 Florence, Italy
17 European Laboratory for Particle Physics, CERN, CH-1211 Geneva 23, Switzerland
18 World Laboratory, FBLJA Project, CH-1211 Geneva 23, Switzerland
19 University of Geneva, CH-1211 Geneva 4, Switzerland
20 Chinese University of Science and Technology, USTC, Hefei, Anhui 230 029, China[△]
22 University of Lausanne, CH-1015 Lausanne, Switzerland
23 INFN-Sezione di Lecce and Università Degli Studi di Lecce, I-73100 Lecce, Italy
24 Institut de Physique Nucléaire de Lyon, IN2P3-CNRS,Université Claude Bernard, F-69622 Villeurbanne, France
25 Centro de Investigaciones Energéticas, Medioambientales y Tecnologícas, CIEMAT, E-28040 Madrid, Spain[♭]
26 INFN-Sezione di Milano, I-20133 Milan, Italy
27 Institute of Theoretical and Experimental Physics, ITEP, Moscow, Russia
28 INFN-Sezione di Napoli and University of Naples, I-80125 Naples, Italy
29 Department of Natural Sciences, University of Cyprus, Nicosia, Cyprus
30 University of Nijmegen and NIKHEF, NL-6525 ED Nijmegen, The Netherlands
31 California Institute of Technology, Pasadena, CA 91125, USA
32 INFN-Sezione di Perugia and Università Degli Studi di Perugia, I-06100 Perugia, Italy
33 Carnegie Mellon University, Pittsburgh, PA 15213, USA
34 Princeton University, Princeton, NJ 08544, USA
35 INFN-Sezione di Roma and University of Rome, "La Sapienza", I-00185 Rome, Italy
36 Nuclear Physics Institute, St. Petersburg, Russia
37 INFN-Sezione di Napoli and University of Potenza, I-85100 Potenza, Italy
38 University and INFN, Salerno, I-84100 Salerno, Italy
39 University of California, San Diego, CA 92093, USA
40 Dept. de Fisica de Particulas Elementales, Univ. de Santiago, E-15706 Santiago de Compostela, Spain
41 Bulgarian Academy of Sciences, Central Lab. of Mechatronics and Instrumentation, BU-1113 Sofia, Bulgaria
42 Laboratory of High Energy Physics, Kyungpook National University, 702-701 Taegu, Republic of Korea
43 University of Alabama, Tuscaloosa, AL 35486, USA
44 Utrecht University and NIKHEF, NL-3584 CB Utrecht, The Netherlands
45 Purdue University, West Lafayette, IN 47907, USA
46 Paul Scherrer Institut, PSI, CH-5232 Villigen, Switzerland
47 DESY, D-15738 Zeuthen, FRG
48 Eidgenössische Technische Hochschule, ETH Zürich, CH-8093 Zürich, Switzerland
49 University of Hamburg, D-22761 Hamburg, FRG
50 National Central University, Chung-Li, Taiwan, China
51 Department of Physics, National Tsing Hua University, Taiwan, China
§ Supported by the German Bundesministerium für Bildung, Wissenschaft, Forschung und Technologie
‡ Supported by the Hungarian OTKA fund under contract numbers T019181, F023259 and T024011.
¶ Also supported by the Hungarian OTKA fund under contract numbers T22238 and T026178.
♭ Supported also by the Comisión Interministerial de Ciencia y Tecnología.
♯ Also supported by CONICET and Universidad Nacional de La Plata, CC 67, 1900 La Plata, Argentina.
♢ Also supported by Panjab University, Chandigarh-160014, India.
△ Supported by the National Natural Science Foundation of China.

Mass Region	$f_2(1270)-a_2(1320)$	$f_2'(1525)$	$f_J(1710)$	Background
Mass (MeV)	1239 ± 6	1523 ± 6	1767 ± 14	–
Width (MeV)	78 ± 19	100 ± 15	187 ± 60	–
Integral (Events)	123 ± 22	331 ± 37	221 ± 55	149 ± 21

Table 1: The parameters of the three Breit-Wigner functions and the parabolic background from the fit on the $K_S^0K_S^0$ mass spectrum.

	$\mathcal{L}(\mathrm{pb}^{-1})$	$\mathcal{K}$ (pb^{-1}/ keV)	ε (%)	$N(f_2')$	$\Gamma_{\gamma\gamma}(f_2') \times \mathrm{Br}(f_2' \to K\bar{K})$ (eV)
Z Pole	143	605	5.0 ± 0.4	42.0 ± 7.8	$83 \pm 15 \pm 12$
High Energies	445	845	6.4 ± 0.5	220 ± 13	$75 \pm 7 \pm 11$

Table 2: The measurement of the two-photon width of the $f_2'(1525)$ for the two data samples. $N(f_2')$ is the integral of the Breit-Wigner function in the $1400 - 1640$ MeV mass region.

	J=0	J=2, $\lambda = 2$	J=2, $\lambda = 0$
Z Pole	$6.0 \pm 0.5\%$	$8.2 \pm 0.7\%$	$4.1 \pm 0.3\%$
High Energies	$6.3 \pm 0.5\%$	$8.7 \pm 0.7\%$	$4.5 \pm 0.3\%$

Table 3: The total detection efficiency for the $f_J(1710)$ for the various spin and helicity hypotheses.

	$\mathcal{K}(\mathrm{pb}^{-1}/\ \mathrm{keV})$	$\varepsilon(\%)$	N_{ev}	N_{bkg}
Z Pole	161	16.6 ± 1.4	6	4.9
High Energies	230	14.2 ± 1.2	36	45.4

Table 4: The $\mathcal{K}$ factor, the detection efficiency ε, the number N_{ev} of observed events and the expected background N_{bkg} for the $\xi(2230)$.

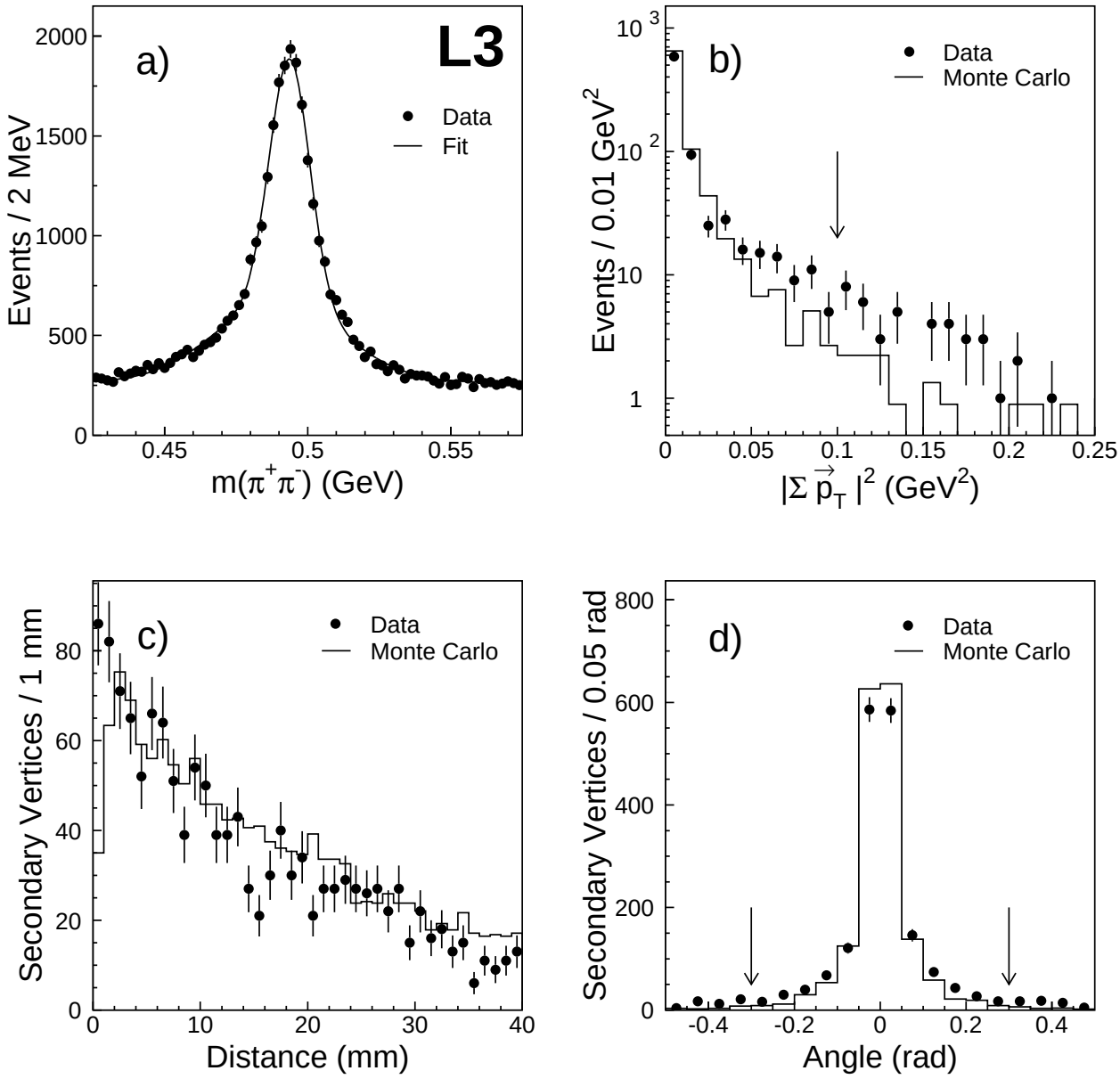

Figure 1: a) The $\pi^+\pi^-$ mass spectrum for reconstructed secondary vertices with a transverse separation of more than 3 mm from the interaction point. b) The total transverse momentum imbalance squared, c) the distance between the primary and the secondary vertex in the transverse plane and d) the angle between the flight direction and the total transverse momentum for the K^0_S candidates. The Monte Carlo predictions correspond only to the signal of $K^0_S K^0_S$ exclusive formation and are normalized to the same area as the data. The arrows indicate the cuts applied.

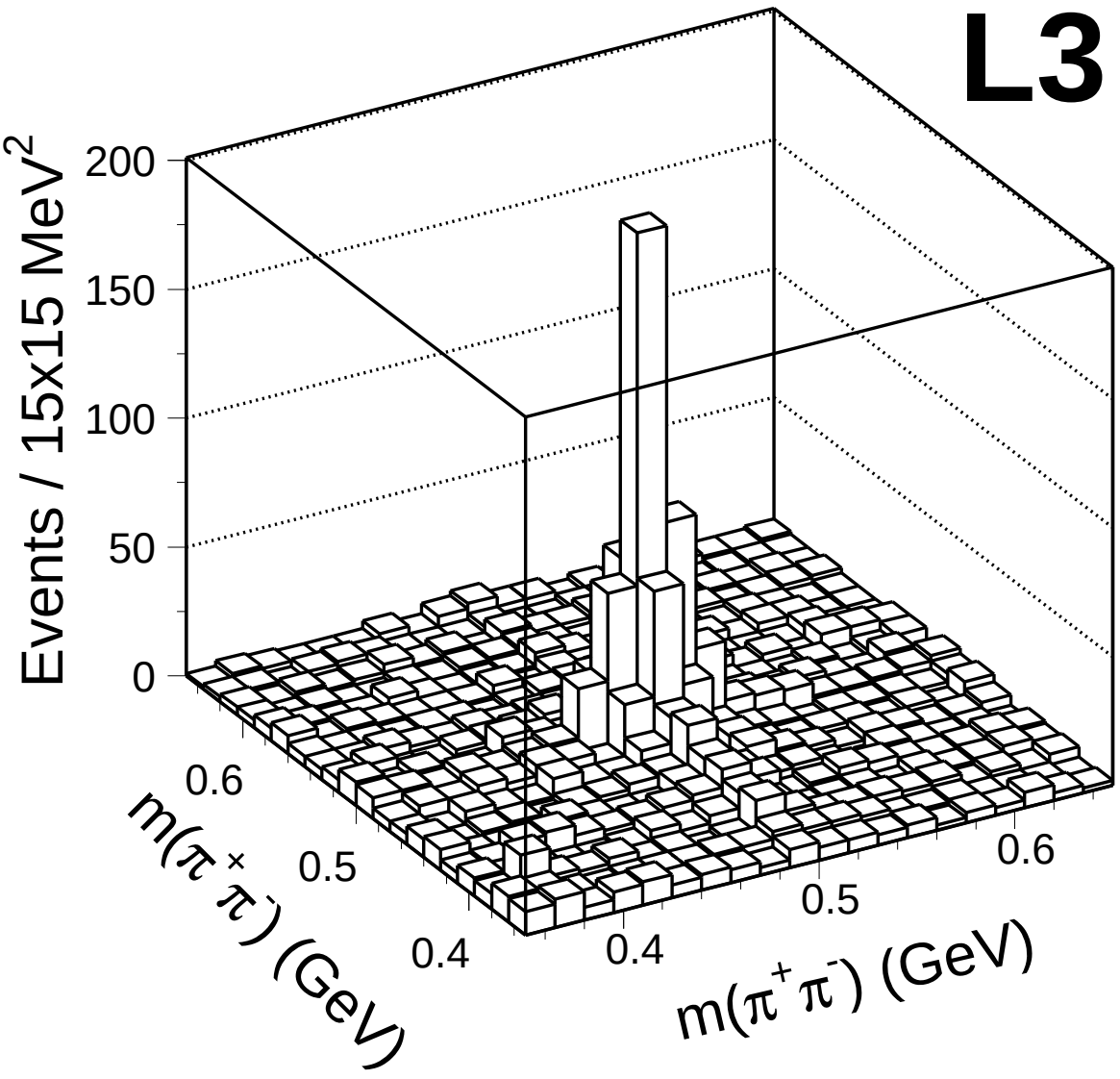

Figure 2: The mass distribution of a K^0_S candidate versus the mass of the other candidate for the full data sample. A strong enhancement corresponding to the $K^0_S K^0_S$ signal over a small background is observed.

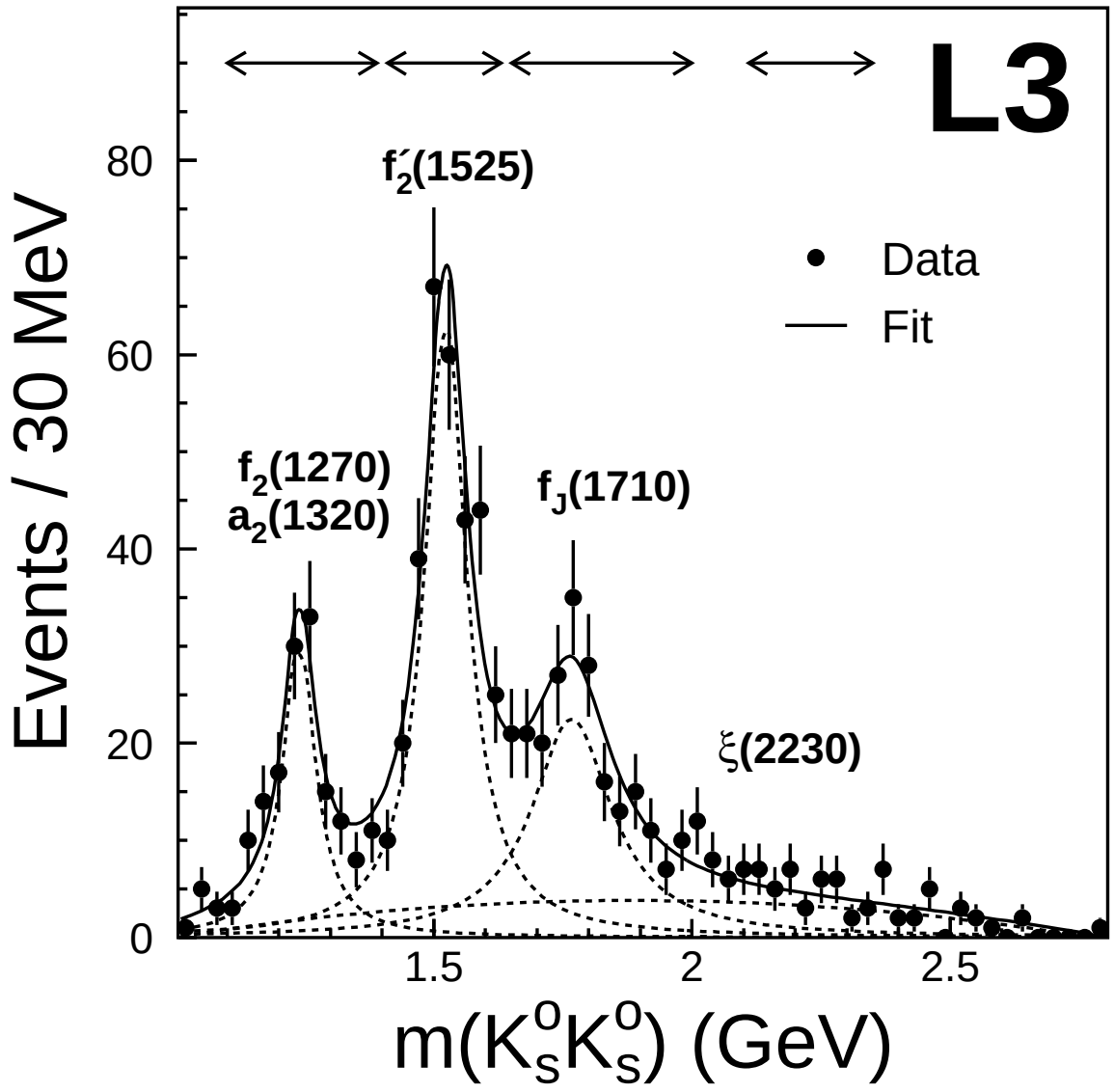

Figure 3: The $K^0_S K^0_S$ mass spectrum: the solid line corresponds to the maximum likelihood fit. The background is fitted by a second order polynomial and the three peaks by Breit-Wigner functions (dashed lines). The arrows correspond to the $f_2(1270)$–$a^0_2(1320)$, the $f'_2(1525)$, the $f_J(1710)$ and the $\xi(2230)$ mass regions.

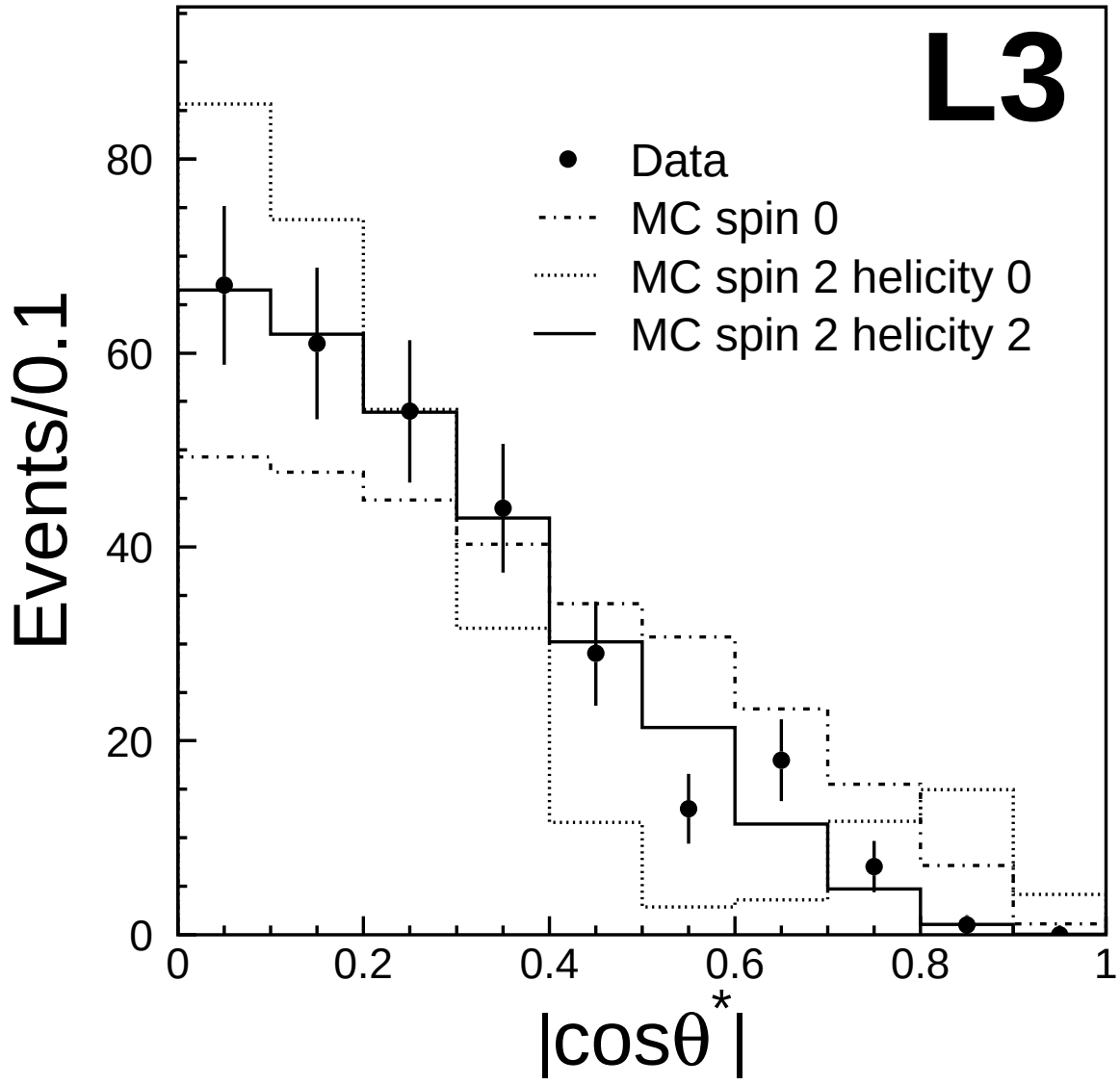

Figure 4: The $K^0_S K^0_S$ polar angle distribution compared with the Monte Carlo distributions for the hypothesis of a pure spin zero, spin-two helicity-zero and spin-two helicity-two states for the $f'_2(1525)$. The Monte Carlo expectations are normalized to the same number of events as the data.

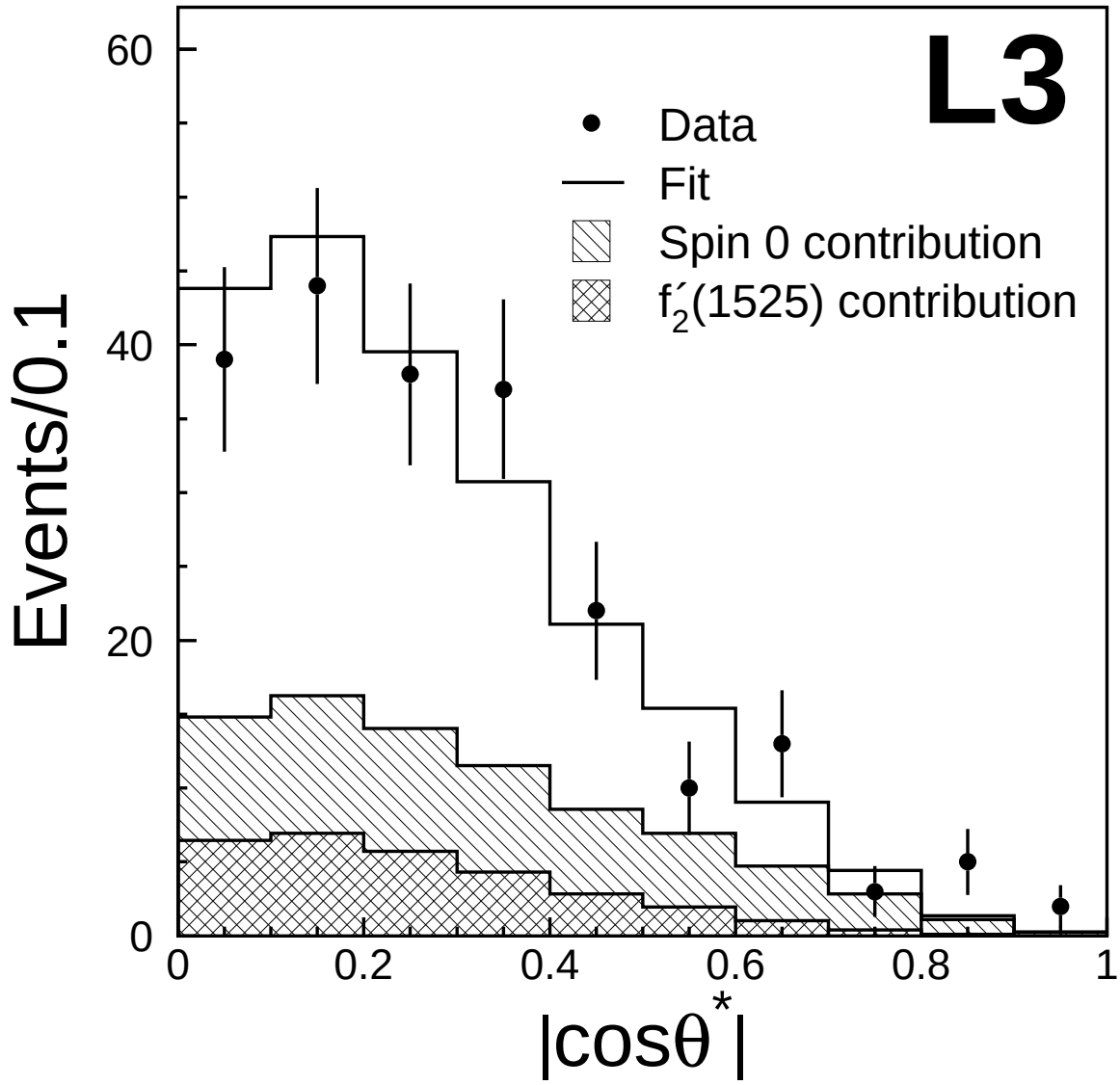

Figure 5: The fit of the $K^0_S K^0_S$ polar angle distribution in the $1640 - 2000$ MeV mass region. The contributions of spin-zero and spin-two helicity-two waves are shown together with the 14% contribution of the tail of the $f_2'(1525)$.